THEORETICAL AND EMPIRICAL EVALUATION OF GEOMETRIC PERFORMANCE OF MULTI-HEAD LARGE FORMAT PHOTOGRAMMETRIC SENSORS

E. Honkavaara, J. Jaakkola, L. Markelin, K. Nurminen, E. Ahokas

Finnish Geodetic Institute, Masala, Finland – (eija.honkavaara, juha.jaakkola, lauri.markelin, kimmo.nurminen, eero.ahokas)@fgi.fi

Commission I, WG I/4

KEY WORDS: Accuracy, Calibration, Camera, Distortion, Geometric, Orientation, Simulation

ABSTRACT:

The geometric performance of large format multi-head photogrammetric sensors, Intergraph DMC and Vexcel UltraCamD, was evaluated theoretically and empirically. Theoretical point determination accuracy coefficients were derived by simulation; point determination accuracy estimates are obtained by multiplying these coefficients by measurement accuracy and scale number. Multi-head images have special multi-head distortions. The simulation study showed that the systematic image distortions caused systematic block deformations. In the empirical study three DMC blocks were evaluated. Point determination accuracy was evaluated using blocks with large overlap percentages. The standard error of unit weight was 2.5-3 μm in adjustments without self-calibration and approximately 2 μm in self-calibrating adjustments; the multi-head parameters efficiently reduced the systematic errors of image residuals. Without additional parameters, the point determination accuracy was 2-4 μm in horizontal coordinates in image and 0.03-0.07‰ of object distance in height; with the best available self-calibration model the corresponding values were 1.5-2 μm and 0.02-0.05‰. Large-scale blocks collected by DMC, UltraCamD and RC20 all gave fairly similar point determination accuracy values. The results indicated that the new digital sensors have great geometric accuracy potential; in order to take full advantage of this potential, appropriate additional parameter models must be developed for each sensor type.

1. INTRODUCTION

Photogrammetric cameras are known for their high geometric accuracy. The high level of accuracy is based on careful manufacturing, which minimizes the geometric errors and maximizes the stability, and on accurate calibration. Despite the careful construction and calibration, systematic geometric errors do occur in the image coordinates. These errors are mainly caused by small remaining inaccuracies and instabilities of the sensor and by non-modeled physical phenomena affecting the entire imaging process. Physical, empirical and mixed additional parameter models have been developed to model the systematic errors (Förstner et al., 2004). These models efficiently compensate the systematic errors in the case of analog systems, and as a consequence, the empirical accuracy of these systems is consistent with theoretical expectations.

The large format photogrammetric sensors are currently constructed using two alternative approaches. The systems are either single-lens systems with linear CCD arrays or multi-head systems with matrix CCD arrays (Cramer 2004; 2005). In this article, the emphasis is on the multi-head systems. At the moment there are two such systems commercially available, Intergraph DMC (Hinz et al., 2000; Tang et al., 2000) and Vexcel UltraCamD (Leberl and Gruber, 2003; Kröpfl et al., 2004).

The geometric evaluations of the multi-head sensors have shown that the virtual images have special systematic distortions, showing a different systematic for each composite image (Honkavaara et al., 2006a, 2006b; Kruck 2006). Results with UltraCamD (Honkavaara 2006b) showed that in order to achieve the highest accuracy additional parameters were needed to compensate the systematic distortions. It also appeared that the conventional additional parameters, assuming a single-head sensor model, were not optimal for the multi-head systems.

The objective of this study is to investigate the geometric performance of UltraCamD and DMC using a strategy based on simulation and empirical evaluations. Materials and methods are described in Section 2. Results are given and discussed in Section 3.

2. MATERIALS AND METHODS

2.1 Materials

Extensive test flights with UltraCamD and DMC were performed at the Sjökulla test field of the Finnish Geodetic Institute (FGI) in 2004 and 2005 (Honkavaara et al., 2006a, b).

The DMC test flights were performed on September 1-2, 2005. The camera was installed in the OH-ACN aircraft used by the National Land Survey of Finland (NLS) utilizing the T-AS gyro stabilized suspension mount. No GPS or GPS/IMU data was collected. In this study, blocks with 5 cm (d1_g5) and 8 cm (d1_g8a, d1_g8b) ground sample distance (GSD) are evaluated. The two blocks with 8 cm GSD were collected on consecutive days to evaluate the stability of the system. Panchromatic large-format images used in the analysis were processed by the DMC Post processing software (Version 4.5). Details of the blocks are given in Table 1 and Figure 1.

Some previously presented UltraCamD and RC20 results are used as reference material (Honkavaara et al., 2006b). In this study, the results of two UltraCamD blocks (u2_g4, u3_g4) collected by two systems in October 2004 and May 2005 are used. Two large-scale analog blocks (r3300, r4000) are used as reference material as well. The reference blocks have a similar structure to the DMC blocks. Some details of the blocks are given in Table 1.

The Sjökulla test field contains approximately 40 targeted ground control points (GCP) with an accuracy of 1 cm in hori-

Table 1. Test blocks

Block	d1_g5	d1_g8a	d1_g8b	u2_g4	u3_g4	r3300	r4000
Date	1.9.2005	1.9.2005	2.9.2005	14.10.2004	14.5.2005	24.4.2004	25.4.2004
GSD (cm)	5	8	8	4	4	6.6	8
Optic (mm)	120	120	120	101.4	101.4	214.108	153.030
Flying height (m)	500	800	800	450	450	710	610
Scale	1:4167	1:6667	1: 6667	1:4440	1:4440	1:3300	1:4000
Swath width (m)	691	1106	1106	460	460	759	920
Overlaps (%)	p=q=60	p=60, q=80	p=60 q=80	p=q=60	p=80, q=60	p=q=80	p=q=60
Strips parallel/cross	6 (+2)/2	4/3	4/-	6/2	4/2	4/4	4/2
Block measurem.	ISAT	ISAT	ISAT	Match-AT	ISAT	SocetSet	SocetSet
Block adjustment	FGIAT	FGIAT	FGIAT	inBlock	inBlock	FGIAT	FGIAT

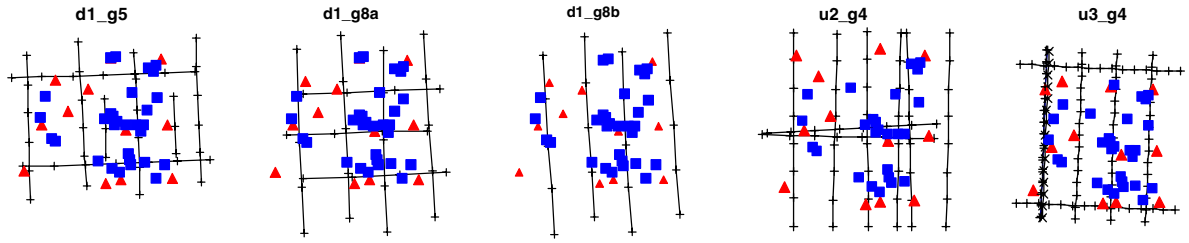

Figure 1. Test blocks. GCPs are marked with triangles and checkpoints are marked with squares.

zontal coordinates and 2 cm in height coordinate. The distribution of the points is shown in Figure 1.

2.2 Methods

A theoretically and practically convenient strategy for evaluating the geometric potential of the photogrammetric sensor consists of the following four phases: 1) evaluation of theoretical geometric performance in the absence of systematic errors, 2) empirical evaluation of the systematic distortions of the images, 3) theoretical evaluation of the effect of the systematic distortions on the quality of the end products, and 4) comparison of empirical results with theoretical results.

2.2.1 Theoretical evaluations. The theoretical performance of the sensors was evaluated by simulation using FGI's own FGIAT software; various block structures, different GCP configurations and the use of auxiliary exterior orientation observations was evaluated. Block accuracy was evaluated both with and without systematic image distortions.

2.2.2 Empirical study. The DMC blocks were measured using Intergraph ISAT software and adjusted using FGIAT software. The UltraCamD blocks were measured using ISAT and Inpho Match-AT software; the block adjustments were performed using Inpho inBlock software (Honkavaara et al. 2006b). Analog blocks were processed with SocetSet and Orima by NLS and adjusted by FGIAT.

The additional parameter models used in this study were the 12 parameter Ebner's model and the 9-parameter physical model (principal point, radial distortion, decentering distortion and in-plane distortion); more details of the models are provided by Förstner et al. (2004) and Honkavaara et al. (2006b). The DMC adjustments were performed using single and multi-head approaches. The single-head approach is the conventional way. In the multi-head approach four different sets of additional parameters were used, one for each component image. The image was divided into four pieces of equal size around the image center. These models are probably not optimal, but they give a possibility to eliminate multi-head distortions into some extent. The additional parameters were treated as weighted observations, allowing a correction in image coordinates of an order of 100 µm. Kruck (2006) has recently discussed the multi-head distortions more thoroughly.

The empirical analysis was performed according to principles described by Honkavaara et al. (2006b). The following quantities were analyzed:

- The camera self-calibration
- The systematic of image observation residuals before and after self-calibration.
- Point determination accuracy before and after self-calibration.

The full blocks and all the GCPs were used in the system calibration. Four parallel strips and 12 GCPs were used in the point determination accuracy evaluation; the rest of the GCPs were used as independent checkpoints (Figure 1). Calculations were performed in a tangential coordinate system; refraction correction was applied.

3. RESULTS AND DISCUSSION

3.1 Theoretical point determination accuracy

DMC and UltraCamD are both multi-head systems. The panchromatic large format DMC image is composed of four sub images of size 4.1 k x 7.2 k, collected by four divergent cameras. The UltraCamD large format image comprises a total of nine 4 k x 2.7 k CCD images, which are also collected by four cameras. Some central parameters of the sensors are given in Table 2; further details are provided by Hinz et al. (2000), Tang et al. (2000), Leberl and Gruber (2003) and Kröpfl et al. (2004).

The digital cameras have a wide field of view (FOV) in the cross-flight direction (y direction), but in the flight direction (x direction) the FOV is smaller. The small FOV in the flight direction reduces the base ratio, which especially decreases the height accuracy. The effects of differences of image formats were analyzed theoretically by simulation.

Table 2. Parameters of sensors

System	f (mm)	Image size (mm) x	Image size (mm) y	Fov (°) x	Fov (°) y	B/Z
Analog	150	230	230	75	75	0.61
Analog	210	230	230	57	57	0.43
DMC	120	92.16	165.888	42	69	0.31
UC	100	67.5	103.5	37	55	0.27

Table 3. Theoretical point determination accuracy

p=60%, q=20%, 13GCP
UC: μ_X =1.2 s σ_0, μ_Y =0.9 s σ_0, μ_Z =3.8 s σ_0
DMC: μ_X =1.3 s σ_0, μ_Y =0.9 s σ_0, μ_Z =3.3 s σ_0
Analog (150 mm): μ_X=1.0 s σ_0, μ_Y= 0.8 s σ_0, μ_Z= 2.1 s σ_0
p=q=60%, 13GCP
UC: μ_X =1.2 s σ_0, μ_Y =0.7 s σ_0, μ_Z =3.0 s σ_0
DMC: μ_X =1.3 s σ_0, μ_Y =0.7 s σ_0, μ_Z =2.5 s σ_0
Analog (150 mm): μ_X=0.9 s σ_0, μ_Y= 0.7 s σ_0, μ_Z= 1.7 s σ_0

3.1.1 Simulation set up. The simulated blocks had four strips with nine images each. Two overlap configurations were evaluated: forward and side overlaps both 60% (p=q=60%), and forward overlap 60%, side overlap 20% (p=60%, q=20%). Each block had three control point configurations: 1) 13 GCPs: one GCP in each block corner and GCPs with 4 base distances in the strip overlap areas, 2) 10 GCPs: one GCP in each block corner and GCPs in the strip overlap areas at the ends of the flight lines, and 3) 4 GCPs: one GCP in each block corner. Calculations were performed with and without GPS/IMU support. In this study 200 mm x 200 mm image format was used for the analog images; for the digital sensors the nominal image sizes were used (Table 2). 30 iterations were performed.

The observations were distorted by normally distributed errors with zero mean. The standard deviations of the generated errors were the following (*pixel* is the pixel size in image):

- Image observations:
  $\sigma_0=\sigma_{tie}=pixel/4$, $\sigma_{GCP\_x}=\sigma_{GCP\_y}=\sigma_{tie}$
  - UltraCamD: σ_{tie}=2.25 µm
  - DMC: σ_{tie}=3 µm
  - Analog: σ_{tie}=5 µm
- GCP ground coordinates:
  $\sigma_{GCP\_X}=\sigma_{GCP\_Y}=\sigma_{GCP\_Z}$= scale factor*$\sigma_{tie}$
- Perspective center observations:
  - $\sigma_{GPS\_X}=\sigma_{GPS\_Y}=\sigma_{GPS\_Z}$=0.1 m
  - $\sigma_{GPS\_X}=\sigma_{GPS\_Y}=\sigma_{GPS\_Z}$= scale factor*$\sigma_{tie}$
- Attitude observations
  $\sigma_\omega=\sigma_\varphi$=0.005°, σ_κ=0.008°

Calculations were performed both without and with systematic image distortions. In the latter case, the average residuals estimated in empirical block adjustments were used as estimates of systematic image distortions (Section 3.2.2).

The simulations produced estimates of the point determination accuracy (average RMSE of the theoretical point determination standard deviations obtained from the normal equation matrix) and estimates of the block deformations (average error at each tie point).

3.1.2 Theoretical coefficients. Theoretical point determination accuracy coefficients were derived from the simulations. In Table 3, the coefficients for the blocks with 13 GCPs are given. By multiplying these coefficients by the scale factor (s) and the point measurement accuracy (σ_0), the point determination accuracy is obtained.

Based on the coefficients it is possible to compare the performance of the sensors. Assuming that the both systems have the same relative image measurement accuracy ($\sigma_0=pixel/n$) and the same GSD, the coefficients show directly the relationship of the point determination accuracy of the systems, because

$$s\sigma_0 = \frac{GSD}{pixel}\frac{pixel}{n} = \frac{GSD}{n} \quad (1)$$

The coefficients (Table 3) were practically the same for both digital sensors for the horizontal coordinates, but DMC had better coefficients for the height accuracy by a factor of 1.1-1.2. This difference is caused by the slightly better base ratio of DMC.

Because DMC has more pixels in the cross-flight direction than UltraCamD, UltraCamD must have larger GSD in order to provide the same swath width as DMC. In the case of the same swath width, the reduction factor for UltraCamD is:

$$\frac{s_{UC}\sigma_{0\_UC}}{s_{DMC}\sigma_{0\_DMC}} = \frac{\frac{swath}{npix_{UC}\cdot pixel_{UC}}\frac{pixel_{UC}}{n}}{\frac{swath}{npix_{DMC}\cdot pixel_{DMC}}\frac{pixel_{DMC}}{n}} = \frac{npix_{DMC}}{npix_{UC}} = 1.2 \quad (2)$$

When this reduction was taken into account in the coefficients of Table 3, it could be concluded that the accuracy of UltraCamD was worse by a factor of 1.1-1.2 in the horizontal coordinates and by a factor of 1.4 in the height coordinate. These factors are representative for the simulated cases only.

3.1.3 Large-scale example. Theoretical point determination accuracy of blocks with 5 cm GSD is shown in Figure 2 (GPS standard deviation 0.1 m, $\sigma_0=pixel/4$). As could be expected on the basis of previous results, the horizontal accuracy of the UltraCamD and DMC was similar. The analog camera had better height accuracy than the digital systems.

3.1.4 Effect of systematic image distortions. The coefficients and rules discussed above hold true only if the observation errors are normally distributed with zero mean. Digital systems have systematic errors, which lower the level of accuracy and cause systematic block deformations. The systematic distortions of DMC images were evaluated in this study (Figure 5; Section 3.2.2). One of the empirical distortion grids (d1_g8a) was used to deteriorate the image observations. Simulations were performed using 5 cm GSD. The blocks were controlled either using 13 GCPs or using 10 GCPs and accurate GPS/IMU support (GPS standard deviation: *scale factor*$*\sigma_{tie}$).

The estimated systematic block deformations are shown in Figure 3. Blocks did not systematically distort when there were no systematic image distortions (Figure 3a, d). Systematic image distortions instead caused block deformations (Figure 3b, e); the deformations were the largest on the block borders. The use of accurate GPS/IMU-observations (Figure 3c, f) and large side overlaps reduced the block deformations (Figure 3f).

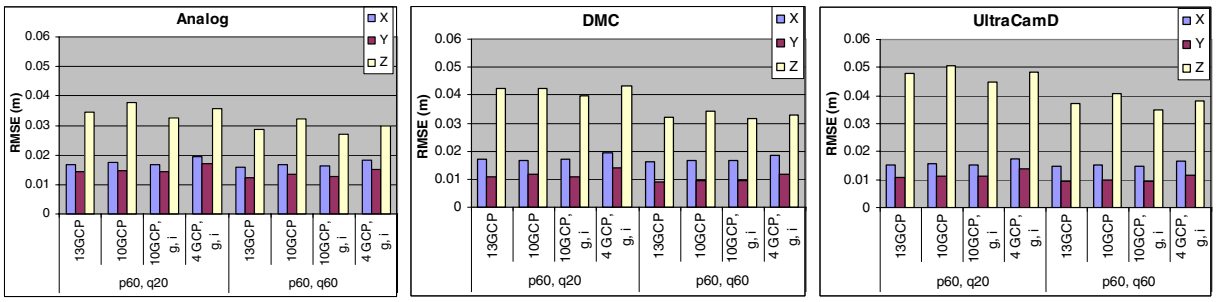

Figure 2. Simulated point determination RMSE. From left to right: analog, DMC, UltraCamD. GSD is 5 cm. (g: GPS, i : IMU)

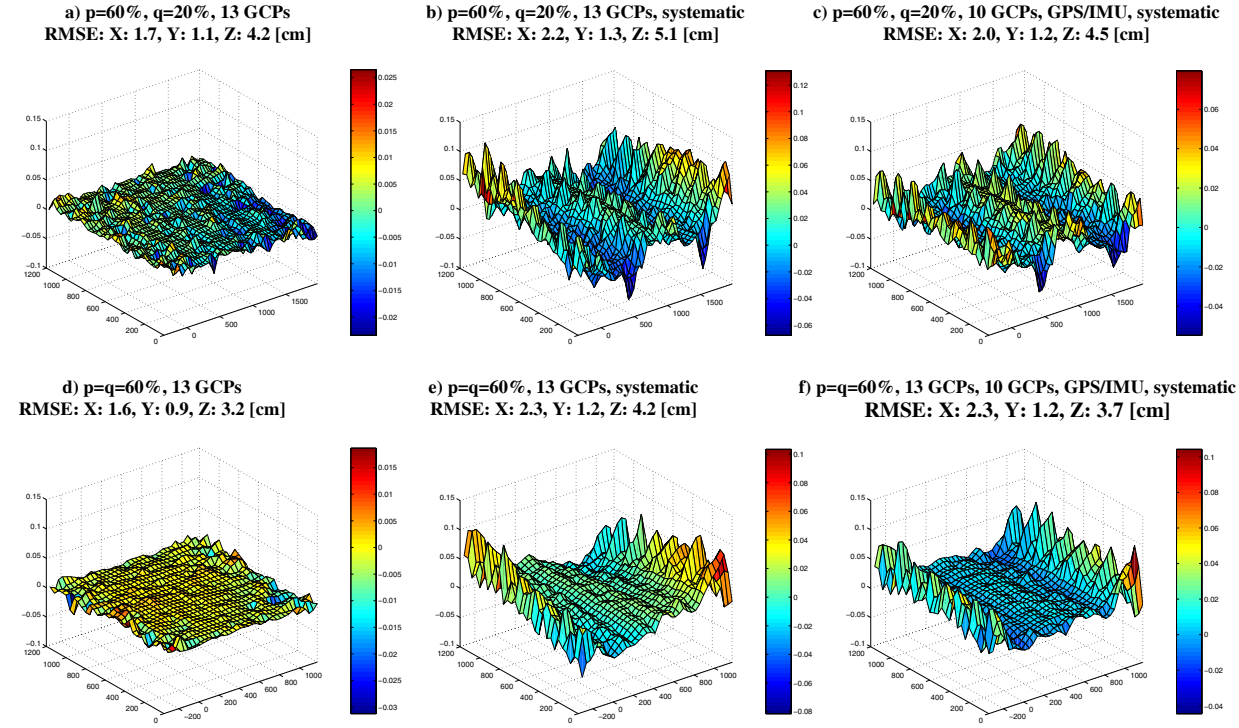

Figure 3. Block height deformations without and with systematic image distortions. The color scale of various cases is different.

This was an example of the use of the simulation in the evaluation of block deformations. The systematic image distortion model was not necessarily correct because it was obtainned from the adjusted image residuals. Similar analysis can be performed with different block structures and distortion models.

3.2 Empirical results

3.2.1 General results. Three types of block adjustment calculations were performed: without additional parameters, with the single-head model and with the multi-head model (Section 2.2.2). The effect of the adjustment model on the standard error of unit weight is shown in Figure 4. When additional parameters were not used, σ_0 was approx. 2.5 µm for the 5 cm GSD block and approx. 3 µm for the 8 cm GSD blocks. With additional parameters σ_0 was approx. 2 µm; the multi-head parameters gave slightly better σ_0 than the single-head parameters.

3.2.2 Systematic of image residuals. Systematic of image residuals was determined by calculating average residuals in a regular 15 x 15 grid; the results are shown in Figure 5. It should be noted that the adjusted residuals do not give the exact magnitude of the systematic distortions; they just show the type and presence of the distortion.

Significant systematic appeared if additional parameters were not used; the maximum average residuals were 6.5 µm and the RMSEs were 1-2 µm. The average residuals for various blocks were correlated. The single-head parameters reduced the systematic only slightly, but the multi-head parameters reduced the systematic effectively. With multi-head physical parameters the maximum average residuals were approx. 2 µm and the RMSEs were 0.55-0.7 µm. The magnitude of the corrections with the multi-head parameters was several pixels.

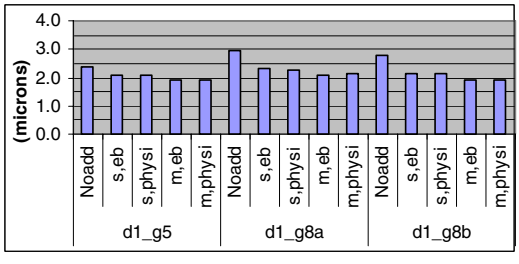

Figure 4. Effect of mathematical model on standard error of unit weight. (Noadd: no additional prameters; eb: Ebner's parameters; physi: physical parmeters; s: single-head model, m: multi-head model)

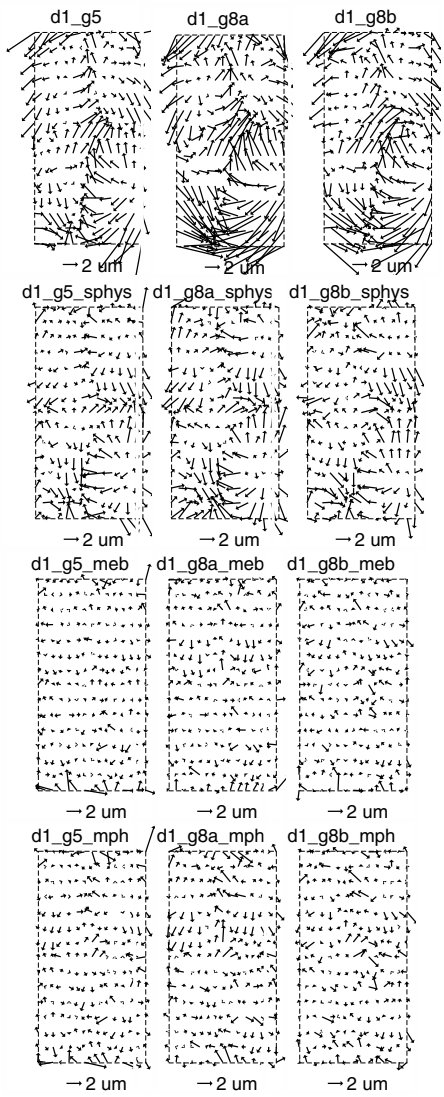

Figure 5. Average residuals of DMC images. First row: without additional parameters. Second row: single-head physical model. Third row: multi-head Ebner's parameters. Fourth row: multi-head physical parameters. Blocks left to right: d1_g5, d1_g8a, d1_g8b.

3.2.3 Point determination accuracy of DMC. Results of the DMC point determination accuracy evaluation (RMSEs at independent checkpoints) are given in Figure 6.

The previous analysis showed that self-calibration reduced the image residuals. Similarly, the point determination accuracy improved in many cases when multi-head additional parameters were used. The Ebner's parameters reduced the empirical accuracy in some cases.

Blocks with 5 cm and 8 cm GSD gave fairly similar accuracy values: approx. 1 cm in horizontal coordinates and 2-3 cm in the height coordinate. One possible reason for the high level of accuracy of the 8 cm GSD block is the higher overlaps. With 5 cm GSD, the accuracy scaled to image was approx. 4 µm in horizontal coordinates and approx. 0.07‰ of object distance (H) in height. With multi-head physical parameters the corresponding numbers were 2 µm and 0.05‰H. With 8 cm GSD the corresponding numbers were approx. 2 µm and 0.03-0.04‰H if additional parameters were not used, and approx. 1.5 µm and 0.02-0.03‰H with the best additional parameter models. The systematic distortions did not appear to cause serious block deformations. However, it should be noted that the test blocks had high side overlaps and dense GCPs, which both reduce the systematic block deformations (Section 3.1.4). Larger deformations could have appeared with weaker block structures.

3.2.4 Comparison of various sensors. Point determination accuracy of the test blocks are presented in Figure 7. The results of blocks u2_g4, u3_g4, r3300 and r4000 were earlier provided by Honkavaara et al. (2006b). All the blocks have four parallel strips and 12 GCPs (Figure 1, Table 1). The multi-head physical additional parameter model was used with DMC. With UltraCamD the single-head physical parameters were used. With RC20 additional parameters were not needed.

UltraCamD was more sensitive to the use of additional parameters than DMC. When the best available model was used, each sensor provided fairly similar object accuracy of 1 cm in horizontal coordinates and 2-4 cm in height.

3.2.5 Comparison of theoretical and empirical values. Only the blocks d1_g5, u2_g4 and r4000 can be compared to the simulated blocks; other empirical blocks have denser GCP distribution and larger overlaps than the simulated blocks (Table 1). The theoretical expectations for block d1_g5 (σ_0=*pixel/6*) were 1.1 cm, 0.6 cm and 2.1 for X, Y and Z, respectively. The corresponding values were 0.8 cm, 0.5 cm and 2 cm for UltraCamD (σ_0=*pixel/6*) and 1.1 cm, 0.8 cm and 2.0 cm for analog camera (σ_0=3 µm). Empirical values of DMC and RC20 were on the same level as the theoretical expectations but the empirical accuracy of UltraCamD was slightly worse than expected. It should be noted that also the limited accuracy of GCPs might distort the empirical values.

Also the theoretical values obtained from the block adjustment (standard deviations of point unknowns) can be compared to the empirical values. The empirical accuracy of DMC and analog camera was better than the theoretical accuracy (Figure 7). Possible explanations for the better than expected empirical accuracy include the higher accuracy of the observations than a priori standard deviations and different distribution of point unknowns and checkpoints. Empirical accuracy of UltraCamD blocks was worse than the theoretical accuracy, especially if self-calibration was not performed.

4. CONCLUSIONS

In this article, the performance of multi-head large format cameras Intergraph DMC and Vexcel UltraCamD has been evaluated theoretically and empirically.

Simulation is an efficient tool for evaluating the performance of various photogrammetric sensors and block structures. If the assumptions made in the simulation are correct, the simulation gives a realistic estimate of the accuracy. Furthermore, the systematic block deformations caused by systematic image distortions can be efficiently evaluated using simulation, as demonstrated in this study. The simulation study showed that slightly better point determination accuracy could be obtained with DMC than with UltraCamD. Stereo plotting geometry of these two sensors is slightly worse than that of wide-angle analog sensors. However, because the accuracy is directly proportional to the image measurement accuracy, the better measurement accuracy of digital images caused by the superior radiometric quality will compensate this difference.

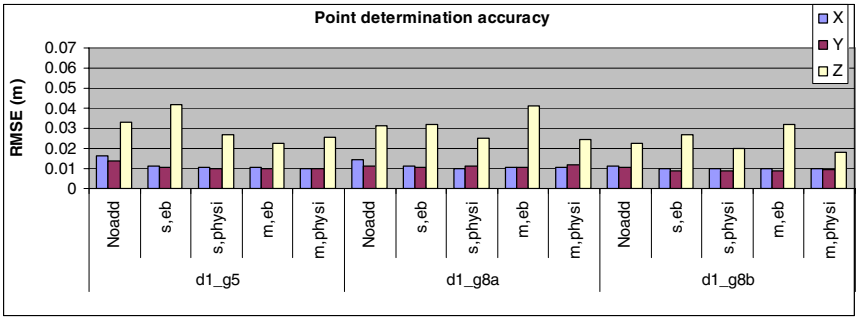

Figure 6. Accuracy of DMC blocks with various additional parameter models. (Noadd: no additional prameters; eb: Ebner's parameters; physi: physical parmeters; s: single-head model, m: multi-head model)

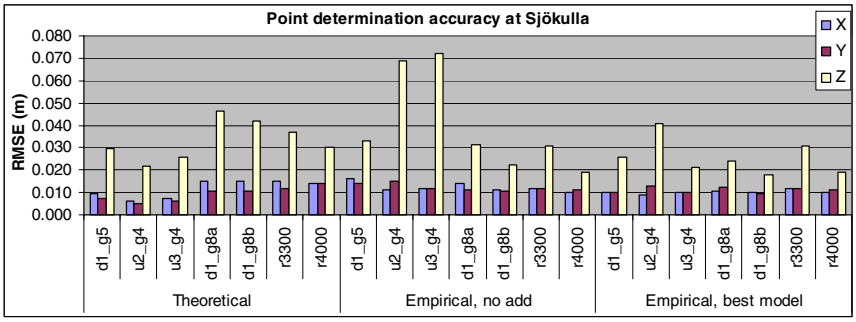

Figure 7. Comparison of point determination accuracy of various blocks collected at the Sjökulla test field.

Large-scale blocks collected by DMC, UltraCamD and RC20 all gave fairly similar point determination accuracy values. The results indicated that the new digital sensors have a great accuracy potential; in order to take full advantage of this potential, appropriate additional parameter models must be developed for each sensor type. The multi-head sensor models used in this study were not optimal, but they clearly demonstrated the importance of appropriate additional parameter models.

ACKNOWLEDGEMENTS

The efforts of several companies and individuals made this study possible. FGI performed the DMC mission in co-operation with the National Land Survey of Finland (NLS). One of the UltraCamD test blocks was a part of a co-operation project carried out by FM-Kartta Ltd, FGI and NLS. Also Finnmap International and NLS provided images for the investigation. The efforts and valuable comments of these companies are gratefully appreciated. The assistance provided by several individuals at the FGI is much appreciated, too.

REFERENCES

Cramer, M., 2004. EuroSDR network on digital camera calibration, Report Phase I (Status Oct 26, 2004). http://www.ifp.uni-stuttgart.de/eurosdr/EuroSDR-Phase1-Report.pdf (accessed May 1, 2006)

Cramer, M., 2005. Digital airborne cameras - status and future. Proceedings of ISPRS Hannover Workshop 2005: High-Resolution Earth Imaging for Geospatial Information, CD-ROM, 8 p.

Förstner, W., Wrobel, B., Paderes, F., Craig, R., Fraser, C., Dolloff, J., 2004. Analytical photogrammetric operations, ASPRS Manual of Photogrammetry, 5th Edition, (J. C. McGlone, E. Mikhail, J. Bethel, Eds.), American Society for Photogrammetry and Remote Sensing, pp. 763-936.

Hinz, A., Dörstel, C., Heier, H., 2000. Digital Modular Camera: System Concept and Data Processing Workflow. International Archives of Photogrammetry and Remote Sensing, Vol 33, Part B2, pp.164-171.

Honkavaara, E., Jaakkola, J., Markelin, L., Peltoniemi, J., Ahokas, E., Becker, S., 2006a. Complete photogrammetric system calibration and evaluation in the Sjökulla test field – case study with DMC, Proceedings of EuroSDR Comm. I and ISPRS Working Group 1/3 Workshop EuroCOW 2006, CD-ROM, 6 p.

Honkavaara, E., Ahokas, E., Hyyppä, J., Jaakkola, J., Kaartinen, H., Kuittinen, R., Markelin, L., Nurminen, K., 2006b. Geometric test field calibration of digital photogrammetric sensors. ISPRS Journal of Photogrammetry and Remote Sensing, Special Issue on Digital Photogrammetric Cameras.

Kruck, E., J., 2006. Simultaneous calibration of digital aerial survey cameras. Proceedings of EuroSDR Comm. I and ISPRS Working Group 1/3 Workshop EuroCOW 2006, CD-ROM, 7 p.

Kröpfl, M., Kruck, E., Gruber, M., 2004. Geometric calibration of the digital large format camera UltraCamD. International Archives of Photogrammetry, Remote Sensing and Spatial Information Sciences 35 (Part B1), 42-44.

Leberl, F., Gruber, M. 2003. Flying the new large format digital aerial camera Ultracam. In: Fritsch (Ed.) Photogrammetric Week 2003, Wichmann Verlag, pp. 67-76.

Tang, L., Dörstel, C., Jacobsen, K., Heipke, C., Hinz, A., 2000. Geometric accuracy potential of the Digital Modular Camera. International Archives of Photogrammetry and Remote Sensing, Vol 33.